Proceedings of 20th International Congress on Acoustics, ICA 2010

23-27 August 2010, Sydney, Australia

Underwater ultrasonic field characterisation using Laser Doppler Vibrometry of transducer motion

Martin Cooling (1), Victor Humphrey (1), Pete Theobald (2) and Stephen Robinson (2)

(1) Institute of Sound and Vibration Research, University of Southampton, Southampton SO17 1BJ, UK.
(2) National Physical Laboratory, Teddington TW11 0LW, UK.

PACS: 43.30.Yj, 43.58.Vb.

ABSTRACT

The full far-field characteristics of an underwater ultrasonic transducer can be predicted from either a 2-D planar scan of the complex pressure in the near-field of the source or a transducer surface velocity scan. A Laser Doppler Vibrometer (LDV) can provide such a scan of the radiating surface and hence has the potential to be a fast, non-invasive method for source characterisation and, in turn, field prediction. Such measurements are, however, significantly complicated by the acousto-optic interaction - that is, the effect on the measurements of the acoustic field through which the laser beam passes. Initial examples of surface velocity measurements and field predictions are presented to show the possibilities of the approach. The results of a theoretical study of the effect of the acousto-optic artefact on LDV measurements for a circular, plane-piston transducer are also presented. The use of a transient pressure field is important both for simulation and experiment, such that measurements are made over a time window which ends before any acoustic signal reaches the water tank boundaries. The simulation results show a significant acousto-optic artefact in the surface velocity data, but also that in spite of this useful field predictions may be made for some applications.

INTRODUCTION

Higher frequency sonar transducers are conventionally characterised by making measurements with hydrophones. For large aperture devices this may require a significant experimental facility in order to reach the far-field, and even then the measurements may not be made at the operational range. One approach is to use a hydrophone to scan a plane (or cylindrical surface) in the near-field of the transducer and propagate this data numerically to predict the far-field behaviour. The propagation of hydrophone pressure scans has already been successfully demonstrated for high frequency sonar transducers [1, 2] and high frequency ultrasound transducers [3, 4]. If required the finite amplitude propagation effects can be accounted for in the propagation step, but such scanning techniques can take a long time for large devices at high frequencies.

However, the development and availability of optical measurement systems, such as Laser Doppler Vibrometers (LDVs), make it possible to consider alternative optical techniques of characterising the fields. For example, an LDV can be used to measure the movement of a thin membrane (pellicle) in the field [5] or used to measure the field by means of the acousto-optic effect [6]. Alternatively, the velocity of the transducer front face may be measured directly, and the 2-D data propagated numerically to predict the acoustic field [2]. This approach, using surface velocity measurement and numerical propagation, enables devices with large near-field regions to be calibrated in small laboratory tanks in principle.

The use of an LDV (or other optical technique) to measure surface velocities in water is, however, complicated by the acousto-optic effect as a result of the pressure wave generated in water. The acoustic wave modifies the apparent optical path length via the acousto-optic effect; the LDV will interpret this change in path length as an additional component of surface velocity. This can be significant, especially for edge waves which propagate across the face of the transducer with their wavefronts parallel to the optical beam, enabling the integrated effect to build up. This has been noted [7, 8] and means that the LDV output will not necessarily be an accurate representation of the surface velocity underwater.

However, the nature of the additional apparent components generated by the edge waves (which appear to propagate across the surface with a phase velocity equal to that of water) means that they will not tend to radiate strongly in the axial direction. The extent to which the additional components are significant is the subject of study; they may not be important for large devices if the real and acousto-optic contributions can be resolved in *k*-space. Results are presented here for the numerical propagation of surface velocity measurements made on large devices, and are confined to small angles from the acoustic axis. In addition results of model predictions are used to further explore the effects of the acousto-optic interaction on field predictions derived from LDV measurements of transducer surface velocity.

PROPAGATION THEORY

Acoustic pressure measurements

Measurements of acoustic pressure made on a transverse plane in front of a transducer can be propagated from one plane to another using a plane wave spectrum approach. This requires the complex pressure $p(x, y, z_0)$ to be measured over the *xy*-plane at a range z_0 from the transducer (see Figure 1).

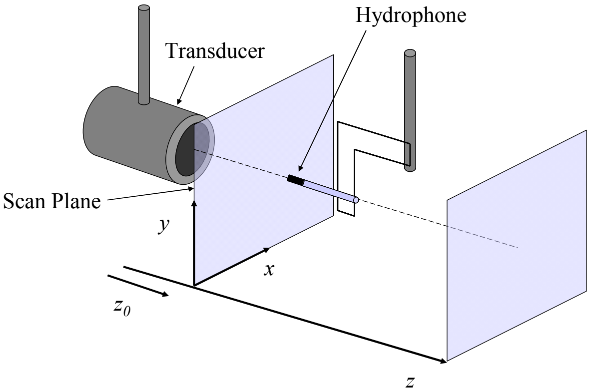

Figure 1. Experimental arrangement for making 2-D hydrophone scans in the near-field of a transducer.

The plane-wave spectrum of the field $P(k_x, k_y)$ can then be calculated by taking the 2-D Fourier transform of the complex pressure [9]:

$$P(k_x,k_y) = \int_{-\infty}^{+\infty}\int_{-\infty}^{+\infty} p(x,y,z_0)\exp\left(-i(k_x x + k_y y)\right)\, dxdy \qquad (1)$$

where k_x and k_y are the components of the wavenumber k along the x and y axes respectively. The pressure distribution in another plane at a different range z can then be calculated by propagating each plane wave component from the measurement plane to the observation plane (by multiplying by an appropriate phase factor) and then performing the inverse 2-D Fourier transform to give the resulting pressure:

$$p(x,y,z) = \left(\frac{1}{4\pi^2}\right)\int_{-\infty}^{+\infty}\int_{-\infty}^{+\infty} P(k_x,k_y)\exp\left(ik_z(z-z_0)\right)\times \exp\left(i(k_x x + k_y y)\right) dk_x dk_y. \qquad (2)$$

Surface velocity measurements

Alternatively, if the transducer is planar and lies in the source plane $r'(x', y', 0)$ and has a normal velocity $v(x', y', 0)$ over its face then the pressure $p(x, y, z)$ at a field point $r(x, y, z)$ can be evaluated, assuming linear propagation, using the Rayleigh integral:

$$p(x,y,z) = \frac{-i\rho_0 c_0 k}{2\pi}\int_{-\infty}^{\infty}\int_{-\infty}^{\infty} v(x',y',0)\frac{\exp\left(ik\left|\mathbf{r}-\mathbf{r}'\right|\right)}{\left|\mathbf{r}-\mathbf{r}'\right|}dx'dy' \qquad (3)$$

where ρ_0 is the water density and c_0 is the speed of sound in the water. An alternative approach is to take the 2-D Fourier transform of the normal velocity to obtain the velocity spectrum in the source plane:

$$V(k_x,k_y,0) = \int_{-\infty}^{\infty}\int_{-\infty}^{\infty} v(x',y',0)\exp\left(-i(k_x x' + k_y y')\right)dx'dy'. \qquad (4)$$

Then the Fourier transform of the pressure in the observation plane at z is given by [9]:

$$P(k_x,k_y,z) = \frac{\rho_0 c_0 k}{k_z} V(k_x,k_y,0)\exp(ik_z z) \qquad (5)$$

where

$$k_z = \sqrt{k^2 - k_x^2 - k_y^2}\,. \qquad (6)$$

Hence the pressure p can be obtained via the inverse Fourier transform.

$$p(x,y,z) = \frac{1}{4\pi^2}\int_{-\infty}^{\infty}\int_{-\infty}^{\infty} P(k_x,k_y,z)\exp\left(i(k_x x + k_y y)\right)dk_x dk_y. \qquad (7)$$

For transducers with dimensions much larger than a wavelength the velocity spectrum will be narrow in k space so that for all k values of significance $k_z \approx k$.

In practice, the pressure distribution or surface velocity is only measured over a limited region of the appropriate xy-plane. This can introduce significant errors unless care is taken to ensure that the pressure/velocity levels are insignificant at the edges of the sampled region. In addition, when performing the forward propagation it is necessary to increase the matrix size by zero padding the measured data to reduce the interference effect resulting from the use of a finite aperture. The use of an FFT results in the measurement aperture being effectively replicated in both the x and y directions; the high angle plane wave components from the replicated apertures can then interfere with the low angle components from the central aperture to give erroneous results. Zero padding the data before taking the 2-D FFT reduces this effect although, in practice, this limits the range achievable by the use of Equations (2) and (7). The far-field behaviour can alternatively be obtained from the plane wave spectrum itself (Equations (1) and (4)) [9].

LDV MEASUREMENT THEORY

Acousto-optic effect

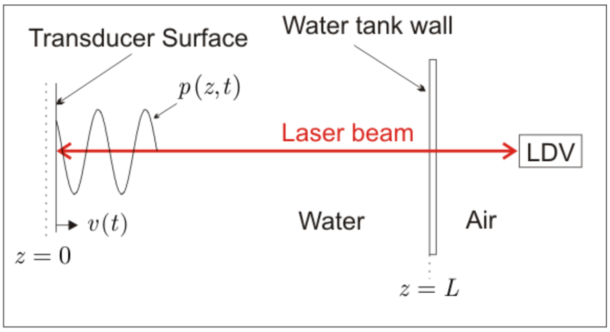

Figure 2. Basic LDV geometry, showing an acoustic pulse having travelled part way to the tank boundary.

Consider a Laser Doppler Vibrometer (LDV) system arranged outside of a water tank so that its laser beam is incident normally on to the surface of the transducer. As a result of the acousto-optic effect the LDV will register an apparent velocity v_{app} where

$$v_{\mathrm{app}}(t) = n_{\mathrm{w}} v(t) - \gamma \frac{\mathrm{d}}{\mathrm{d}t}\left\{\int_0^L p(z,t)\mathrm{d}z\right\} \qquad (8)$$

and γ is the adiabatic piezo-optic coefficient and n_w is the refractive index of water under ambient conditions. The Piezo-optic coefficient describes the changes in optical refractive index with acoustic pressure:

$$\gamma = \left(\frac{\partial n_W}{\partial p}\right)_S. \qquad (9)$$

The special case where the acoustic field is a plane wave that has not propagated as far as the tank window is now considered. Consider the transducer to be stationary at time zero, and then to instantaneously start to move with a perfect sinusoidal velocity:

$$v(t) = v_0 \sin(\omega_0 t), \quad t \geq 0, \\ = 0, \quad t < 0. \tag{10}$$

This results in a pressure

$$p(t) = p_0 \sin(\omega_0 t - kz), \quad t \geq 0, \quad z < c_0 t \\ = 0, \quad t < 0. \tag{11}$$

Here ω_0 is the acoustic angular frequency, k is the acoustic wavenumber in water and $p_0 = \rho_0 c_0 v_0$. For this plane wave case it can be shown [10] that

$$v_{\mathrm{app}}(t) = n_{\mathrm{eff}} v(t) \tag{12}$$

where

$$n_{\mathrm{eff}} = n_{\mathrm{w}} - \gamma \rho_0 c_0^2 = 1.009. \tag{13}$$

For a real transducer the wavefield will not be planar in nature. In addition it is essential to consider the source being driven with a toneburst so that measurements are still made under free-field conditions where the acoustic field hasn't reached the optical window. For this reason it is necessary to model the acousto-optic effect for a time dependant field radiated by a transducer.

Numerical modelling

In order to investigate the effects of the acousto-optic effect on LDV measurements a numerical model was set up to simulate a circular transducer driven with a tone burst signal.

The first step in the calculation process involved calculating the time dependent pressure field $p(r, z, t)$ of a circular transducer, of radius a, through which the laser beam passes. This was achieved using a method described by Stepanishen [11] which expresses the velocity potential at a point in space as a convolution of the transducer impulse response with the source velocity time history. This was used to calculate the wavefield as a function of time at each spatial co-ordinate (r, z).

These results were then used to calculate the apparent velocity of the transducer using Equation (8) by numerically integrating along the laser path at a constant radial coordinate r. The calculated values were numerically differentiated to give the temporal derivative of the integrated pressure, again as a function of time. From this the effective transducer velocity, as would be seen by a LDV, was calculated.

The fundamental signal measured by an LDV is the time-dependent apparent velocity considered thus far. Commercial LDVs are, however, often designed to measure steady-state surface vibration. This is achieved by taking the Fourier transform of an appropriately time-gated section of the raw velocity signal, resulting in a measured velocity spectrum. Data at individual frequency components are then typically assessed by viewing 2D amplitude and phase distributions. For underwater transducer measurement, it will be the velocity spectrum component at the driving frequency that is of interest.

Such steady-state measurements have been simulated by processing the apparent velocity signals predicted by the numerical model in exactly the same way. The only real decision to make regarding the simulation of steady-state results is what time window to use. This was selected to simulate that typically used in experimental measurements.

EXPERIMENTAL MEASUREMENTS

Hydrophone Measurements

Example results that show the potential of the LDV technique will be considered in this section.

The measurements reported here were performed on a circular transducer 200 mm in diameter at a frequency of 500 kHz. It was chosen because it had a near-field region that extended to a significant distance; however, the transition to the far-field occurred at a distance that was still accessible within a 5.5 m diameter large open tank at NPL.

The transducer was driven with a tone-burst, derived from an arbitrary waveform generator and amplified by an ENI 240L power amplifier. Near-field scans were performed in a small 2 m x 1.5 m x 1.5 m GRP test tank with a two carriage positioning system. This tank also featured a glass window to allow the LDV system to interrogate the transducer and acoustic field. The 'far-field' measurements were made in a large open, wooden test tank, 5.5 m in diameter and 5 m deep and at a larger reservoir facility.

Near-field hydrophone scans of the field were undertaken by scanning a Reson TC4035 hydrophone over a planar surface in the acoustic near-field, with the amplitude and phase of the signal being measured at discrete points and the received signals analysed using a HP89410A vector signal analyser with on-board spectral analysis. The tone burst length, analysis window length and window start time were selected with care to ensure that complete information about the transducer surface vibration was obtained at all points on the measurement scan. Scans were automated, enabling them to be left overnight to complete. Step sizes were chosen to be $\lambda/2$ or smaller to ensure that the Nyquist sampling criterion was satisfied and the scan width was chosen to ensure that the signal amplitude was at least 20 dB lower at the scan edges than that at the beam centre.

LDV Measurements

Optical scans of the transducer were undertaken using a Polytec PSV-300 scanning vibrometer, consisting of an OFV 056 scanning head and a PSV-Z-040-F control unit. The vibrometer scanned the laser beam over a grid of user defined positions on a surface and measured the normal component of the surface velocity by measuring the Doppler shift of the reflected laser light.

The vibrometer was positioned 0.834 m outside the small open tank (2 m x 1.5 m x 1.5 m), with the optical beam entering the tank via a glass window. The transducer was positioned 0.58 m from the window, providing a total optical stand-off distance of around 1.6 m assuming a refractive index of 1.33 for water. The vibrometer provided a measurement range of ±250 mm s^{-1}.

The vibrometer scan was synchronised with the function generator with 5 averages being performed for each scan point. The output of the vibrometer was then band-pass filtered to isolate the frequency of interest. A spatial scan resolution of approximately 1 mm was used and the total scan angle never exceeded 7.5°.

EXPERIMENTAL RESULTS

A scan of the acoustic pressure amplitude, in the x-y plane of the transducer at a range of 10 mm, is shown in Figure 3(a). This can be compared with a scan of surface velocity made with the LDV in Figure 3(b). It should be noted that this transducer has two concentric annular active regions that vibrate with different amplitudes; in addition both results clearly show that it has a defect at the top edge of the inner region. The similarity of these two plots indicates that the LDV measures a surface velocity distribution that is similar to the pressure very near to the transducer surface. The LDV data does, however, appear to have a poorer resolution than the hydrophone data; the reason for this has not so far been identified.

(a)

(b)

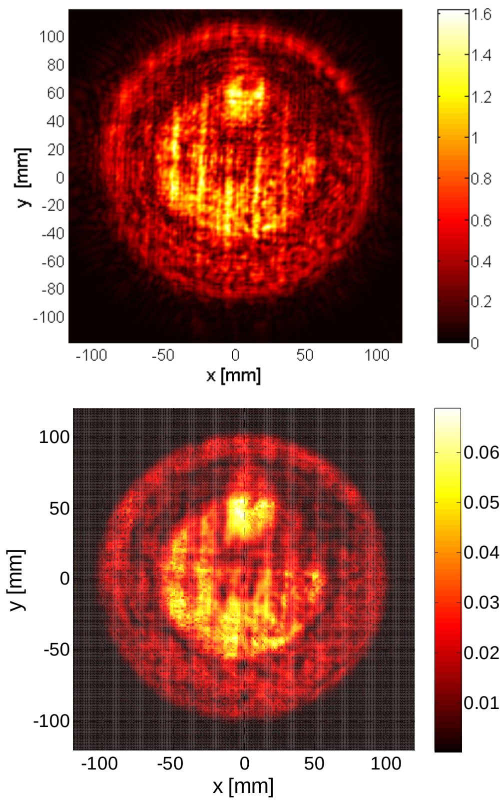

Figure 3. Results for (a) pressure amplitude measured at 10 mm from the transducer face and (b) direct measurement of the surface velocity amplitude using a scanning LDV (linear scale).

The result of propagating the LDV data by taking the velocity spectrum, calculating the pressure spectrum at a distance and then calculating the pressure distribution using the inverse FFT is shown in Figure 4(c). This shows the magnitude of the field in the transverse *xy*-plane at a range of z = 3.34 m on a dB scale, normalised to the maximum value. For comparison Figure 4(b) shows hydrophone data obtained conventionally at 3.34 m on the same 0 to -40 dB range. The excellent agreement should be noted. (The non-ideal nature of the source results in the rather complex field shown.)

The result of propagating the near-field hydrophone scan shown in Figure 3(a) to 3.34 m is shown in Figure 4(a). Clearly the propagated pressure and optical data produce similar beam cross-sectional data at this range.

(a)

(b)

(c)

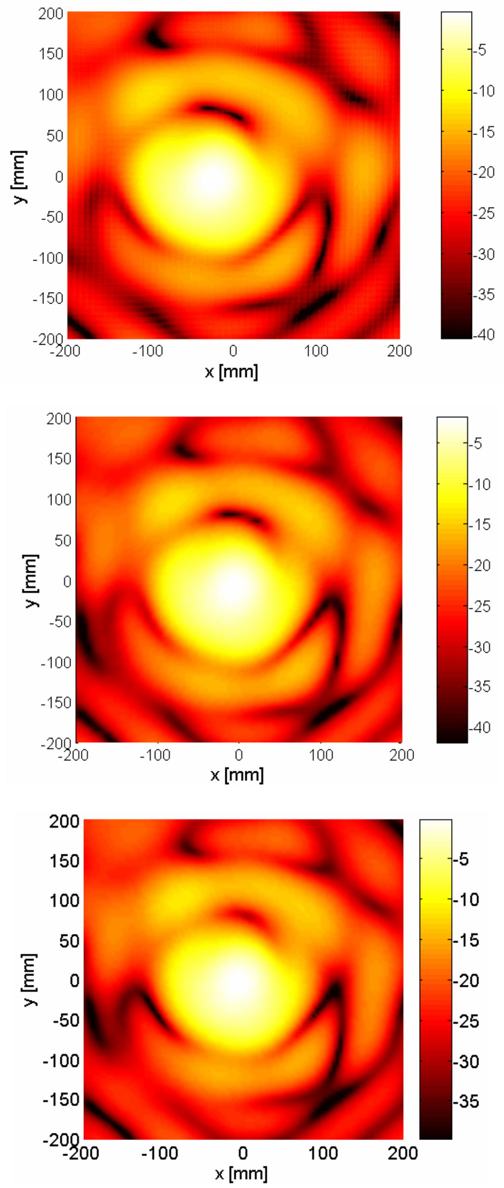

Figure 4. Normalised pressure amplitude results (in dB) in the *xy*-plane for the 500 kHz transducer at 3.34 m showing: (a) forward-propagated pressure field from 10 mm, (b) direct measurement at 3.34 m, and (c) forward-propagated optical LDV surface velocity measurements.

Figure 5(a) shows a quantitative comparison of the numerically propagated LDV data and a measured beam-plot in the $y = 0$ plane at 3.34 m. Good agreement is shown between the measured beam profile and the predicted profile generated by forward propagating the optical data. The main lobe is reproduced very well, but some departures are evident in the side lobes. These can be attributed, in part, to the fact that the transducer had to be transferred to the larger tank to make the 3.34 m measurements, making it difficult to ensure consistency of vertical alignment between the measurements in different tanks. A similar comparison for a range of 24.4 m is shown in Figure 5(b). Again the agreement for angles up to 10º is very good, although that for higher order sidelobes is not as good. The extent to which this is a result of alignment issues is not clear.

The results of these experiments imply that optically measured surface velocity data can be used as an input to numerical propagation routines to predict the far-field characteristics of transducer fields. However, it is clear that optical LDV measurements are subject to artefacts due to the acousto-optic effect. In order to investigate this further the numerical modelling of the acousto-optic effect for a real transducer field needs too be considered.

(a)

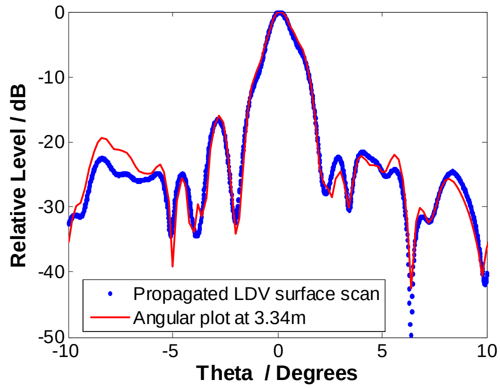

(b)

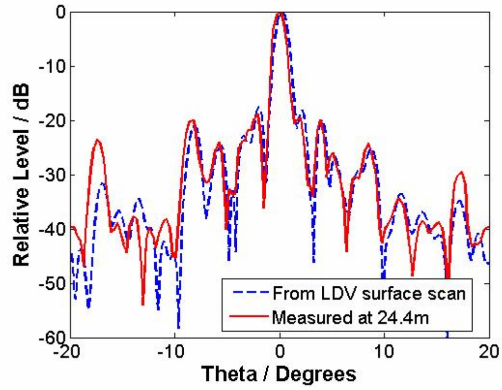

Figure 5. Measured beam plots for 500 kHz transducer at (a) 3.34 m and (b) 24.4 m. Measurements are compared with the results predicted by linear propagation of the LDV scan data.

MODEL SIMULATIONS

Model predictions were run for a much smaller device (31.75 mm in diameter) at 500 kHz. Figure 6 shows the magnitude and phase of the apparent velocity that would be measured by a LDV, as a function of the radial coordinate, according to the model. The magnitude is normalised by the true velocity, which is also shown for comparison. This shows clear deviations from the true velocity over the transducer surface with a particularly large deviation on the acoustic axis. For $r>a$, i.e. over the baffle surrounding the piston, the apparent velocity is not zero, and only falls off slowly with r. The phase variation indicates that the apparent velocity looks like a wave that travels over the surface of the baffle with the speed of sound in water.

In order to understand more of this behaviour it is possible to subtract the expected velocity from the apparent velocity to obtain the optical artefact in the velocity (OA_{EW}). Figure 7 shows the normalised magnitude and phase of this artefact velocity, again as a function of the radial coordinate. Over the transducer area the artefact has the appearance of a standing wave in a system with circular symmetry; the acousto-optic artefact appears to be dominated by the effect of the edge wave propagating over the surface of the transducer. This is because in this region the wavefronts and the laser beam are parallel so the effect of the acousto-optic effect can build up constructively.

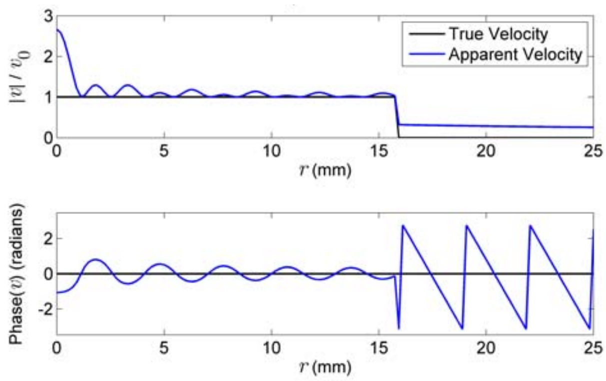

Figure 6. Simulated steady-state apparent velocity and true surface velocity for a 15.9 mm radius circular piston source. All amplitudes and phases are expressed relative to those of the true surface velocity over the radiating area.

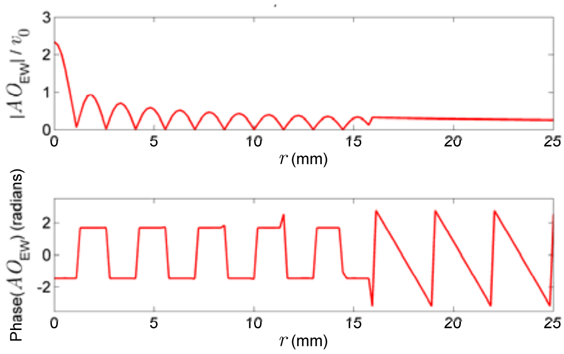

Figure 7. Velocity artefact (apparent velocity – true velocity) for the results presented in Figure 6. All amplitudes and phases are expressed relative to those of the true surface velocity over the radiating area.

These results indicate how the acousto-optic effect will make it difficult to analyse transducer surface vibration underwater using LDV techniques. However, it is possible to use the simulated LDV data as input to a propagation routine to predict the far-field beam pattern (using Equation (7)). The resulting normalised directivity is shown in Figure 8, with the true directivity of a circular piston for comparison. This shows that the beam pattern is very well reproduced for angles up to 30º, with only the nulls between the sidelobes not well reproduced. However the directivity predictions above 50º show significant deviations from the true directivity, especially as the angle approaches 90º.

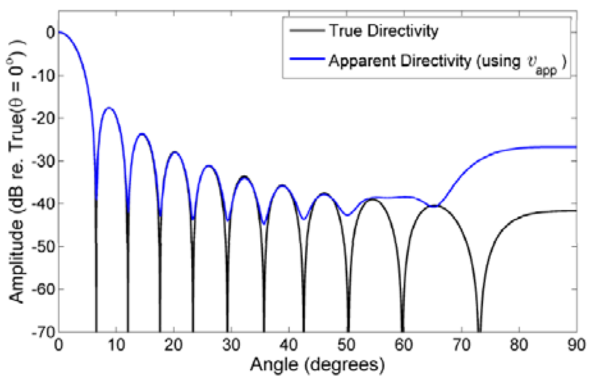

Figure 8. Predicted far-field directivities calculated from the simulated apparent velocity distribution for a 15.9 mm radius, 500 kHz circular piston transducer. The true directivity is shown for comparison.

This result emphasises that the acousto-optic artefact mainly affects the directivity results at high angles. This can be attributed to the fact that the principle contribution to the surface velocity artefact is associated with the edge waves that travel across the transducer and baffle with a velocity c_0. As a consequence the velocity artefact has a peak in its plane wave spectrum at 90º, although the artefact spectrum extends to lower angles because of the finite size of the region on the transducer and baffle for which the velocity data is available and can be analysed.

DISCUSSION AND CONCLUSIONS

The results presented show that in principle an LDV system can be used to obtain 2D scans of surface velocity for ultrasonic transducers underwater. These may be used in a similar way to hydrophone scan data as an input to a linear propagation model to derive the pressure field at other distances and far-field directivities. Experimental results for a large (200 mm diameter) 500 kHz transducer show good agreement between the two approaches for angles near the acoustic axis. The optical approach has the potential advantages over hydrophone scans of being non-perturbing, higher resolution and faster.

However, the radiated pressure field has the potential to create extra phase shifts via the acousto-optic effect which the LDV interprets as an additional apparent velocity of the surface [7, 8].

Model simulations show that this velocity artefact can be comparable with the true velocity, and is mainly associated with the edge waves that travel across the surface of the transducer and surrounding baffle. Clearly this makes the interpretation of LDV data for a transducer in water difficult, especially as the effects may resemble what might be expected from standing waves on the transducer surface.

However, simulated LDV data for a small transducer, 31.75 mm in diameter, has been used to calculate the far-field directivity from the apparent surface velocity. This shows that the effect of the artefact on the propagated field directivity is small for angles up to 30º, confirming the experimental observations that indicate that it is possible to estimate far-field directivities for small angles from LDV data. Further detailed calculations are currently being used to investigate the acousto-optic effect for tone bursts and the factors affecting LDV measurements of ultrasonic transducer surface velocities underwater.

ACKNOWLEDGEMENT

The authors would like to acknowledge the support of the Acoustics and Ionising Radiation Programme at the National Physical Laboratory (part of the Department for Business, Innovation and Skills National Measurement System).

REFERENCES

1 V.F. Humphrey, S.P. Robinson, P.D. Theobald, G. Hayman, P.N. Gélat and A.D. Thompson, “Comparison of optical and hydrophone-based near-field techniques for full characterisation of high frequency sonar” *Proceedings of Underwater Acoustic Measurements*, Heraklion, Crete, Greece, 457-464 (2005).
2 V.F. Humphrey, G. Hayman, S.P. Robinson and P.N. Gélat, “Forward and back propagation of wavefields generated by large aperture transducers” *Proceedings of the Seventh European Conference on Underwater Acoustics, ECUA 2004*, Delft, The Netherlands, 1045-1050 (2004).
3 M.E. Schafer and P.A. Lewin, “Transducer characterisation using the angular spectrum method” *J. Acoust. Soc. Am.* **85**, 2202-2214 (1989).
4 P.R. Stepanishen and K.C. Benjamin, “Forward and backward projection of acoustic fields using FFT methods” *J. Acoust. Soc. Am.* **71**, 1158-1164 (1982).
5 P.D. Theobald, S.P. Robinson, A.D. Thompson, R.C. Preston, P.A. Lepper and Y.B. Wang, “Technique for the calibration of hydrophones in the frequency range 10 to 600 kHz using a heterodyne interferometer and an acoustically compliant membrane” *J. Acoust. Soc. Am.* **118**, 3110-3116 (2005).
6 A.R.Harland, J.N. Petzing and J.R. Tyrer, “Non-perturbing measurements of spatially distributed underwater acoustic fields using a scanning laser vibrometer” *J. Acoust. Soc. Am.* **115**, 187-195 (2004).
7 O.A. Sapozhnikov and A.V. Morozov, “Piezoelectric transducer surface vibration characterisation using acoustic holography and laser vibrometry” *2004 IEEE International Ultrasonics, ferroelectrics and Frequency Control Joint 50th Anniversary Conference* (2004).
8 D. Certon, G. Ferin, O. Bou Matar, J. Guyonvarch, J.P. Remenieras and F. Patat, “Influence of acousto-optic interactions on the determination of the diffracted field by an array obtained from displacement measurements” *Ultrasonics* **42**, 465-471 (2004).
9 E.G. Williams, *Fourier Acoustics: Sound Radiation and Nearfield Holography*, Academic Press (1999).
10 C.B. Scruby, and L.E. Drain, *Laser Ultrasonics*, Adam Hilger, Bristol (1990).
11 P.R. Stepanishen, “Transient radiation from pistons in an infinite planar baffle” *J. Acoust. Soc. Am.* 49, 1629-1638 (1971).